Dendritic Ca^{2+} signalling due to activation of α7-containing nicotinic acetylcholine receptors in rat hippocampal neurons

Dmitriy Fayuk and Jerrel L. Yakel

Laboratory of Neurobiology, National Institute of Environmental Health Sciences, National Institutes of Health, Department of Health and Human Services, PO Box 12233, Research Triangle Park, NC 27709, USA

Neuronal nicotinic acetylcholine receptors (nAChRs) are in the superfamily of Cys-loop ligand-gated ion channels, which are widely expressed in the brain. Among the many different subtypes of nAChRs known to be expressed in the rat brain, the α7-containing nAChRs are considered to be the most permeable to Ca^{2+}. Utilizing highly localized and rapid iontophoretic agonist delivery, combined with patch-clamp electrophysiology and fura-2 fluorescence imaging techniques, we examined the α7 nAChR-mediated currents and $[Ca^{2+}]_i$ transients in the dendrites of rat hippocampal CA1 interneurons in the slice. We found that in the dendrites, whereas the amplitudes of the current responses were smaller and the decay kinetics faster than the responses in the soma, the amplitudes of the $[Ca^{2+}]_i$ signals were significantly larger. Cultured hippocampal neurons were studied since the dendritic field lies in the same focal plane, which allowed for a broader investigation of the spatiotemporal dynamics of $[Ca^{2+}]_i$ signalling. In cultured neurons, the $[Ca^{2+}]_i$ signals in the dendrites were similar to those in slices. Interestingly in cultures, even though the amplitude of the α7 nAChR-mediated currents dramatically decreased with distance from the soma (from ~20–250 μm), the amplitude of the $[Ca^{2+}]_i$ signals did not correlate with distance. This indicates that the relative efficacy of α7 nAChR activation to increase $[Ca^{2+}]_i$ levels in dendrites increased severalfold with distance from the soma. These results may have implications for the role that α7 nAChRs have in regulating various signal transduction cascades, synaptic plasticity, and memory processes, via significant changes in $[Ca^{2+}]_i$ levels.

(Resubmitted 25 April 2007; accepted 14 May 2007; first published online 17 May 2007)
Corresponding author J. L. Yakel: NIEHS, F2–08, PO Box 12233, 111 T. W. Alexander Drive, Research Triangle Park, NC 27709, USA. Email: yakel@niehs.nih.gov

Neuronal nicotinic acetylcholine receptors (nAChRs) are in the superfamily of Cys-loop ligand-gated ion channels that are widely expressed in the brain. Thus far, at least 11 different nAChR subunits are currently known to be expressed in the rat. Functionally, nAChRs are cationic channels, and different subtypes of neuronal nAChRs are known to be differentially permeable to Ca^{2+} (Bertrand *et al.* 1993; Séguéla *et al.* 1993; Fucile, 2004; Dani & Bertrand, 2007). Thus, nAChRs have the capacity to elicit local changes in cytoplasmic calcium ($[Ca^{2+}]_i$) levels, which has implications for regulating various signal transduction cascades, synaptic plasticity, and memory processes (Berg & Conroy, 2002; Quick & Lester, 2002; Dajas-Bailador & Wonnacott, 2004; Fucile, 2004). For example, the influx of Ca^{2+} through α7 nAChRs in either chick ciliary ganglion (CG) or cultured rat hippocampal neurons can activate Ca^{2+}-dependent signal transduction cascades and changes in gene expression (Chang & Berg, 2001; Hu *et al.* 2002). However this influx of Ca^{2+} can also have deleterious consequences by causing excitotoxicity, in particular at endplate nAChRs, which has been linked to various neuromuscular diseases including congenital myasthenic syndromes (CMS; Engel & Sine, 2005; Fucile *et al.* 2006). In addition, the rapid desensitization of α7-containing nAChRs may prevent Ca^{2+} overload and neurotoxicity since the expression of a mutant form of this channel, which results in dramatically reduced desensitization, enhances neurotoxicity (Lukas *et al.* 2001).

The hippocampus is a region of the brain known to be important for cognition and working memory (Levin, 2002; Dani & Bertrand, 2007), where nAChRs can directly regulate synaptic plasticity (Hunter *et al.* 1994; Fujii & Sumikawa, 2001; Ji *et al.* 2001; McGehee, 2002). In the rat hippocampus, GABAergic interneurons receive

 DOI: 10.1113/jphysiol.2007.135319

cholinergic input from the medial septum–diagonal band complex (MSDB) of the basal forebrain (Frotscher & Léránth, 1985; Woolf, 1991), and express diverse subtypes of somato-dendritic nAChRs. The nAChRs in the hippocampus are divided into two major groups, the α7-containing and non-α7 receptors, and the α7-containing nAChRs are generally considered to be the most permeable to Ca^{2+} in the rat brain (Bertrand *et al.* 1993; Séguéla *et al.* 1993; Castro & Albuquerque, 1995; Fucile, 2004).

Calcium-dependent signal transduction cascades themselves can affect the function of α7-containing nAChRs. For example, α7-containing nAChRs in chick CG neurons are regulated by the Ca^{2+}-dependent phosphatase calcineurin (CaN) and the Ca^{2+}-dependent kinase CaMKII (Liu & Berg, 1999). In addition on somatic spines of these chick CG neurons, the α7-containing nAChRs undergo rapid activity-driven, Ca^{2+}-dependent trafficking that requires functional SNAREs (Liu *et al.* 2005). In rat hippocampal interneurons, we recently described a novel form of Ca^{2+}-dependent potentiation of α7-containing nAChRs which may be involved in regulating synaptic plasticity in the hippocampus; this phenomenon was enhanced by dialysing cells with peptide inhibitors of either calcineurin or PKC, and was attenuated by dialysing cells with the CaMKII inhibitor KN-93 (Klein & Yakel, 2005).

Because of the importance of the Ca^{2+} signalling and regulation of nAChRs in the hippocampus as it relates to cognition and synaptic plasticity, it is critical to understand the function and regulation of nAChRs in these neurons in a physiological setting such as the slice. Furthermore dendrites are complex integrators of chemical and electrical signals (Goldberg & Yuste, 2005), yet it is unknown how dendritic nAChRs are regulating Ca^{2+} signalling in the hippocampus or elsewhere. To do this, we combined patch-clamp electrophysiology recordings with conventional fura-2 fluorescence imaging techniques to measure the changes in $[Ca^{2+}]_i$ levels in the dendrites of rat CA1 hippocampal interneurons in slices, and activated the nAChRs utilizing highly localized and rapid iontophoretic agonist delivery. Recently we reported that the activation of somatic α7-containing nAChRs elicited a modest increase in somal $[Ca^{2+}]_i$ transients (Fayuk & Yakel, 2005). Here we have investigated $[Ca^{2+}]_i$ signals in the dendrites, which interestingly were larger than in the soma even though the amplitude of the currents were smaller. Cultured hippocampal neurons were studied since this allowed for a broader investigation of the spatiotemporal dynamics of $[Ca^{2+}]_i$ signalling, and since $[Ca^{2+}]_i$ signals were similar to those in slices. In these cultures, even though the amplitude of the α7 nAChR-mediated currents dramatically decreased with distance from the soma, surprisingly the amplitude of the $[Ca^{2+}]_i$ signals did not correlate with distance. Therefore, the relative efficacy for the activation of the α7 nAChRs to increase $[Ca^{2+}]_i$ signals in dendrites increased with distance from the soma. We will discuss the implications that these results may have concerning the role of α7 nAChRs in various Ca^{2+}-dependent signal transduction cascades and synaptic plasticity.

Methods

Slice preparation

All experiments were carried out in accordance with guidelines approved by the NIEHS Animal Care and Use Committee, which includes minimizing the number of animals used and their suffering. Standard techniques were used to prepare 350 μm thick acute hippocampal slices from 14- to 21-day-old-rats (Fayuk & Yakel, 2004). Briefly, rats were anaesthetized with halothane (Sigma) and decapitated. Brains were quickly removed and placed into an ice-cold oxygenated, artificial cerebral spinal fluid (ACSF) containing (mM): 119 NaCl, 2.5 KCl, 1.3 $MgCl_2$, 2.5 $CaCl_2$, 1 NaH_2PO_4, 26.2 $NaHCO_3$, and 11 glucose. After dissection, brain chunks were glued to the stage of a vibrating microtome (VT1000S; Leica, Nussloch, Germany) for slicing while immersed in the cooled oxygenated ACSF. Slices were placed onto nylon mesh immersed in oxygenated ACSF at room temperature and then used for recordings within about 6 h, and after at least 1 h of recovery period.

Culture preparation

Dissociated rat hippocampal cell cultures were prepared according to modified plating protocol described by Gibco (Invitrogen Corporation). Briefly, hippocampal tissue was dissected from embryonic day 18–19 Sprague–Dawley rats and triturated with fire-polished Pasteur pipettes in Hanks' balanced salt solution (HBSS) without divalent cations (i.e. $HBSS^-$). Cells were transferred to HBSS with divalent cations (i.e. $HBSS^+$) and spun for 1 min at 200 RCF. The supernatant was discarded and the pellet was resuspended in $HBSS^+$, and aliquots were added to 24-well plates containing poly L-lysine-coated round (12 mm) glass coverslips and 1 ml of plating media (see below). Cultures were incubated at 35°C and 95% air–5% CO_2 humidified atmosphere for 4–6 weeks before experiments, and half of the media was exchanged twice a week with media (plating media but without glutamic acid). $HBSS^-$ was supplemented with 1 mM sodium pyruvate, 50 units ml^{-1} penicillin, 50 $\mu g\,ml^{-1}$ streptomycin, and 10 mM Hepes (pH 7.4); $HBSS^+$ has in addition Ca^{2+} and Mg^{2+}. Plating medium consisted of Neurobasal medium with 0.5 mM glutamine, 25 μM glutamic acid and 2% B-27 supplement added. All solutions, media and supplements are from Gibco.

Electrophysiology and iontophoresis

Whole-cell patch-clamp recordings were performed on CA1 interneurons from the stratum oriens in slices, or cultured rat hippocampal neurons. Patch pipettes (Garner 7052 or 8250 glass, with resistances of 3–4 MΩ) were filled with a solution that contained (mM): 120 caesium gluconate, 2 NaCl, 4 Na_2ATP, 0.4 Na_2GTP, 4 $MgCl_2$ and 20 Hepes (pH 7.2–7.3). Slices were superfused at room temperature (18–22°C) with ACSF. Synaptic activity and muscarinic AChRs were blocked with TTX (1 μM) and atropine (1 μM) added to the ACSF. Cells were clamped using an Axopatch 200B amplifier (Axon Instruments, Union City, CA, USA) at a holding potential of −70 mV, and currents were recorded and analysed using pCLAMP software (Axon Instruments); recordings were analysed only if the holding current was less than 100 pA. To deliver agonists to the cell via iontophoresis, double-barrelled glass pipettes (∼20 MΩ) pulled from theta glass pipette (Harvard Apparatus, USA; o.d. = 2 mm) on a P-97 micropipette puller (Sutter Instruments, Novato, CA) were filled with ACh (1 M) and choline (1 M) and placed ≤ 5 μm from the surface of the soma or dendrites, and then positive current pulses (200 nA, 20–100 ms) were applied using an Axoclamp-2A amplifier (Axon Instruments). For the precise localization of injection pipette tip and parts of studied neuron, Alexa Fluor 488 (hydrazide sodium salt; Invitrogen) was added to solutions filling the patch (20 μM) and injection (100 μM) electrodes. Drugs studied were diluted at final concentrations in ACSF and were delivered to the cell through a gravity-fed multichannel perfusion system ending with a non-metallic syringe needle (250 μm ID, WPI) placed just above the slice surface to ensure the homogenous coverage of the area surrounding the cell being studied.

Imaging of $[Ca^{2+}]_i$

Changes in intracellular Ca^{2+} levels ($[Ca^{2+}]_i$) in the soma and dendrites in response to either ACh or choline were assessed with conventional fura-2 fluorescence imaging techniques using an Eclipse E600FN upright microscope (Nikon, Japan) with a 60× fluorescent water-immersion objective, a Lambda DG-4 light source (Sutter Instrument Company, USA) equipped with a stabilized xenon arc lamp (175 W) and four-channel filter interchange system, and an iXon cooled (−75°C) 14-bit digital camera (Andor Technology, UK). The iQ imaging software (Andor Technology) was utilized to acquire and store images for off-line analysis, and to synchronize with membrane current recordings. Fura-2 pentapotassium salt (200 μM; Invitrogen) was dialysed into the cell via the patch pipette, and its fluorescence was alternately excited with 340 and 380 nm light. Pairs of images were recorded at 5–10 Hz with 25–50 ms exposure for each excitation wavelength using a 510 nm emission filter. In each cell tested, background fluorescence was monitored until it stabilized (usually by 10–20 min) prior to recordings. A region of interest was selected and the 340/380 ratio of fluorescence intensities corrected for background signal were calculated using the imaging software. The ratio values were then converted to $[Ca^{2+}]_i$ levels according to the calibration curve obtained with the *in vitro* Ca^{2+} calibration procedure using the Ca^{2+} calibration kit (Molecular Probes). This procedure consisted of measurements of the 340/380 ratio in solutions containing 11 different Ca^{2+} concentrations from 0 to 39 μM; the ratio value for 0 μM was 0.44, and for 39 μM was 8.4. Statistical analyses were performed using Origin software (OriginLab Corp., Northampton, MA, USA). Averaged data were presented as means ± S.E.M., and statistical significance was tested using an ANOVA.

Calculation of relative Ca^{2+} efficacy

We estimated the relative efficacy for the activation of the α7 nAChRs to increase $[Ca^{2+}]_i$ signals by calculating the 'Ca^{2+} index'; this is the ratio of the increase in $[Ca^{2+}]_i$ (to $\geq$ 80% of maximal amplitude) to the integrated membrane current (charge, Q) induced by the activation of these channels. We limited the time of current integration to the fast phase of the $[Ca^{2+}]_i$ rise to minimize integration of the current provided by receptor activation in neighbouring regions due to diffusion of agonist, in order to diminish the underestimation of I_{Ca}.

Results

Iontophoretic activation of α7 nAChRs on the soma of rat hippocampal interneurons induces rapid current responses

Recently we reported that the activation of somatic α7 nAChRs by pressure-applied agonist on rat CA1 hippocampal interneurons induced Ca^{2+} influx sufficiently large to induce significant $[Ca^{2+}]_i$ transients in the soma (Fayuk & Yakel, 2005). Here we have investigated whether dendritic α7 receptors respond similarly. We measured changes in inward currents and $[Ca^{2+}]_i$ signals in the dendrites of these interneurons utilizing iontophoresis to apply agonists (ACh and choline; see Methods) since pressure application of agonists produced significant physical disturbance to the dendrites such that it was not feasible to accurately measure $[Ca^{2+}]_i$ signals without artifacts. Iontophoretic pulses (up to 200 nA and 100 ms in duration) did not cause any detectable tissue movement, and had the added advantage of a more focal activation of nAChRs (see below).

In acute slices of the CA1 region of rat hippocampus, brief (5–100 ms) iontophoretic (200 nA) applications of either ACh, or the α7 nAChR-selective agonist choline (Papke et al. 1996), to the soma of voltage-clamped CA1 stratum oriens interneurons elicited rapidly activating and decaying inward currents (Fig. 1). Previously we have shown that fast choline- and ACh-induced responses are completely blocked by the α7-selective antagonist methyllycaconitine (MLA; Fayuk & Yakel, 2004). In the present study, ACh and choline responses in dendrites (which were always fast-activating, i.e. with 10–90% peak rise-times of < 100 ms) were completely blocked by MLA (25 nM; data not shown). The average amplitude, rise-time, and half-time of decay for whole-cell inward currents induced by the iontophoretic application of choline (200 nA, 100 ms) were 957 ± 160 pA, 15 ± 3 ms and 100 ± 12 ms, respectively (15 cells).

In some cells, we compared responses induced by both the iontophoretic and pressure application of agonist. We found that the iontophoretic application of choline near the soma activated currents that were similar in amplitude and rise-time to the currents induced by the pressure application of a maximal dose of choline (10 mM for 50–100 ms; Fig. 1*B*). However, the responses due to pressure-applied choline usually decayed more slowly for the later phases of the response decay (Fig. 1*B*). This slowness of decay is likely to be due to the greater diffusion of the agonist, which can subsequently result in the

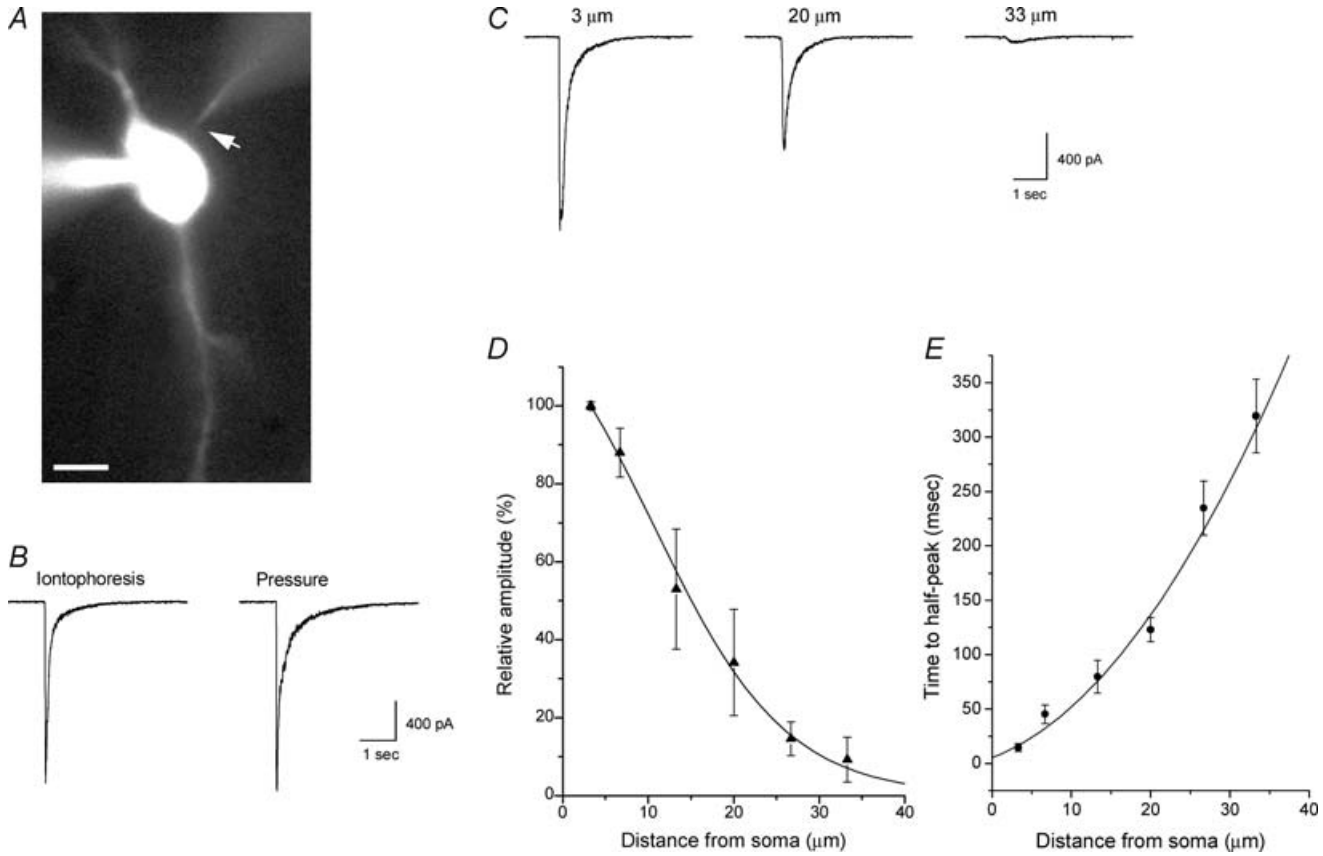

Figure 1. Iontophoretic choline application induces rapid and focal activation of α7 nAChRs in rat hippocampal interneurons in the slice

A, fluorescence image of a patch-clamped rat CA1 interneuron from the stratum oriens in an acute hippocampal slice. Both the patch and iontophoretic electrodes contained Alexa Fluor 488 (20 μM and 100 μM, respectively) and can be visualized; the iontophoretic electrode is located in close proximity to the soma (arrow). The scale bar is 10 μm. *B*, brief iontophoretic choline application (100 ms, 200 nA, 1 M choline in iontophoretic electrode) and pressure application of choline (10 mM, 100 ms, right trace) near the soma ($\sim$3–5 μm; left trace) induced similar rapid inward currents in the same cell. *C*, the amplitude and kinetics of the inward currents activated by the iontophoretic application of choline were dependent on the distance between the tip of the iontophoretic electrode and the soma. The relative amplitude (as a percentage of the response amplitude at a distance of 3 μm) of the responses at variable distances is plotted in *D* (5 cells), and the data have been fitted to a Gaussian function. The time required to activate responses at variable distances is plotted in *E*; values plotted are the elapsed time from the initiation of the iontophoretic pulse until the current reached half of the peak amplitude (i.e. time to half-peak).

greater activation of receptors at more distal regions of the cell.

To assess the focal nature of the iontophoretic application of agonists in our experiments, we applied choline (200 nA, 100 ms) to the soma from variable distances (Fig. 1*C*) and plotted the relative amplitude of activated currents (as a percent of maximal response) *versus* distance from the soma. Fitting a Gaussian function to the data yielded a half-width value of ∼15 μm (5 cells; Fig. 1*D*). In addition, we estimated the rate of diffusion of choline from the tip of the iontophoretic electrode by plotting the time required from the initiation of the iontophoretic pulse until the activated current reached half of the peak amplitude (i.e. time to half-peak). This value ranged from 15 ± 4 ms at a distance of ∼3 μm to 320 ± 30 ms at a distance of ∼33 μm (Fig. 1*E*). Together these data suggest that under our experimental conditions, the iontophoretic application of choline can near-maximally and rapidly activate α7-containing nAChRs in a manner that is consistent with the spatially restricted activation of these receptors.

Iontophoretic activation of α7 nAChRs on dendrites induces local $[Ca^{2+}]_i$ signals

The iontophoretic application of choline (200 nA, 100 ms) to the dendrites of rat hippocampal CA1 interneurons (approximately 30–100 μm away from the soma; Fig. 2) induced inward currents with average amplitude, rise-time and half-time of decay values of 330 ± 60 pA, 15 ± 2 ms and 56 ± 10 ms, respectively (18 cells). The amplitudes of dendritic responses were smaller and the decay kinetics significantly faster ($P < 0.05$) than the currents activated in the soma. This reduction in current amplitude in dendrites is consistent with what was observed for the local photolysis of caged carbachol in hippocampal interneurons (Khiroug *et al.* 2003).

In addition to activating inward currents, iontophoretic choline application on the dendrites induced local $[Ca^{2+}]_i$ transients. The average amplitude, rise-time and half-time of decay values for the $[Ca^{2+}]_i$ signals for the dendritic region nearest to the tip of the iontophoretic electrode (within 5 μm) were 34 ± 10 nM, 220 ± 30 ms and 1.4 ± 0.2 s, respectively (18 cells; Fig. 2*B* and *C*). Interestingly, the amplitudes of the $[Ca^{2+}]_i$ signals in the dendrites were significantly larger than that previously observed for $[Ca^{2+}]_i$ signals in the soma (Fayuk & Yakel, 2005). In order to estimate the relative efficacy of α7 nAChR activation to increase $[Ca^{2+}]_i$ levels in dendrites, we calculated the 'Ca^{2+} index'; this is the ratio of the amplitude of the $[Ca^{2+}]_i$ signal to the concurrent integrated membrane current (charge, *Q*) (see Methods). The mean value of the Ca^{2+} index for the activation of the α7 receptors in the dendrites was 900 ± 210 M C^{-1} (18 cells).

The iontophoretic application of ACh to dendrites induced fast-activating α7 nAChR-mediated currents and $[Ca^{2+}]_i$ signals similar to choline in peak current amplitude (302 ± 30 pA), $[Ca^{2+}]_i$ changes (28 ± 7 nM), rise-times of currents (15 ± 2 ms) and $[Ca^{2+}]_i$ signals (270 ± 20 ms), as well as the half-time of current decay (72 ± 9 ms); however, the half-time of decay of the ACh-induced $[Ca^{2+}]_i$ signals (2.1 ± 0.1 s; 32 cells) was significantly slower than for choline (i.e. 1.4 s).

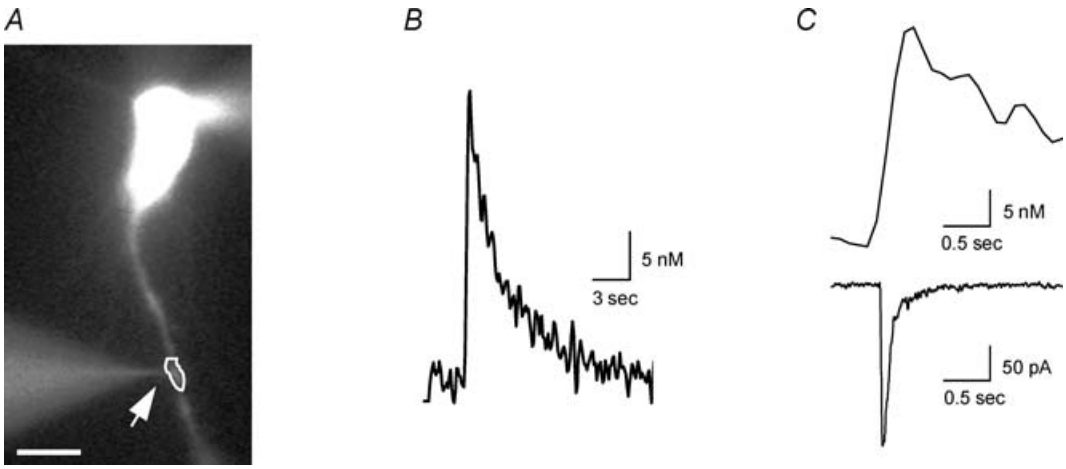

Figure 2. Iontophoretic activation of α7 nAChRs in dendrites induces $[Ca^{2+}]_i$ signal and current
A, fluorescence image of a patch-clamped neuron tested with choline iontophoretic application in close proximity to the dendrite (arrow). The scale bar is 10 μm. *B*, the $[Ca^{2+}]_i$ signal from dendritic region denoted in *A* detected using fura-2 fluorescent imaging techniques. *C*, both the $[Ca^{2+}]_i$ signal (top) and current (bottom) induced by choline iontophoretic application from region in *A* (note different time scale from *B*).

Temporal and spatial aspects of dendritic $[Ca^{2+}]_i$ signals due to the activation of α7 nAChRs

In order to establish whether $[Ca^{2+}]_i$ signals are limited to the dendritic region adjacent to the site of choline application, or are propagated along the dendrite, we examined the spatiotemporal characteristics of the dendritic α7 nAChR-mediated $[Ca^{2+}]_i$ signals. Pseudo-coloured images of the changes in $[Ca^{2+}]_i$ levels in the dendrite clearly show that the spread of the $[Ca^{2+}]_i$ signals occur in both directions away from the site of stimulation (Fig. 3*A*). By plotting the temporal changes in $[Ca^{2+}]_i$ levels along the dendrites at different distances from the tip of the iontophoretic electrode, we observed the wave-like propagation of the $[Ca^{2+}]_i$ signal with decreasing amplitude from the stimulation site (Fig. 3*C*). For the dendritic region nearest the iontophoretic electrode (i.e. point 'c' for this dendrite; Fig. 3*C*), a detectable $[Ca^{2+}]_i$ signal was already observed on the first image captured at 100 ms after choline application, and peaked by 200 ms. For distant locations along this dendrite (i.e. ~10–15 μm away for points 'b' and 'd', and ~25–30 μm away for points 'a' and 'e'), the $[Ca^{2+}]_i$ signals peaked by 300 ms and 700 ms, respectively. The peak of the $[Ca^{2+}]_i$ signal was not only delayed with distance, but also was decreased to ~85–90% of maximal amplitude for points 'b' and 'd', and to ~40–50% for points 'a' and 'e'.

We plotted the relative amplitude of the $[Ca^{2+}]_i$ signals (as a percentage of maximal response from the point nearest to the tip of the iontophoretic electrode) from nine dendritic locations in different cells *versus* time after the iontophoretic application of choline, for variable distances from the tip of the iontophoretic electrode (Fig. 3*D*). For the point nearest the iontophoretic electrode, the $[Ca^{2+}]_i$ signals peaked in ~400 ms, whereas at a distance of 10 μm, 20 μm, and 30 μm, the $[Ca^{2+}]_i$ signals did not peak until ~550 ms, 700 ms and 800 ms, respectively. The peak of the $[Ca^{2+}]_i$ signal also was decreased to ~80%, 55% and 30%, respectively, at distances of 10 μm, 20 μm and 30 μm. The delay with distance along the dendrite in the time-to-peak $[Ca^{2+}]_i$ signal, as well as the decrease in peak $[Ca^{2+}]_i$ level with distance, is consistent both with the apparent rate and extent of diffusion of choline from the tip of the iontophoretic electrode (Fig. 1*D* and *E*).

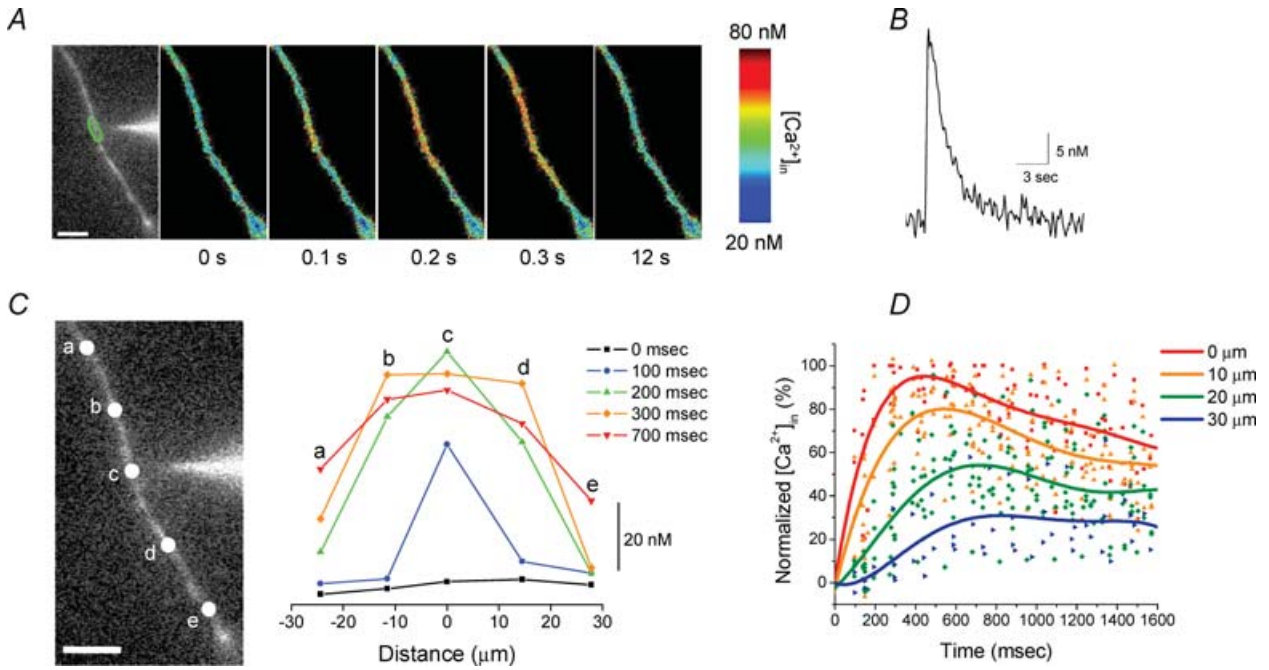

Figure 3. Temporal and spatial distribution of the dendritic α7 nAChR-mediated $[Ca^{2+}]_i$ signals
A, fluorescence image with iontophoretic electrode in close proximity to the dendrite (left image), and pseudo-colour images at different time points show the spread of the increase in $[Ca^{2+}]_i$ level and recovery induced by iontophoretic choline application. *B*, the $[Ca^{2+}]_i$ signal from dendritic region denoted in *A*. *C*, the changes in $[Ca^{2+}]_i$ levels from five different locations for the dendrite in *A* (left image) were plotted at different time points (right; each line corresponds to the same time point as noted in the legend). *D*, summary of data obtained from similar experiments in 9 cells. The changes in $[Ca^{2+}]_i$ levels for dendritic regions at variable distances (i.e. 0, 10, 20 and 30 μm) away from the tip of the iontophoretic electrode were plotted as a percentage of the maximal amplitude for the point nearest to the iontophoretic electrode (i.e. 0 μm) *versus* time after the iontophoretic application of choline. The data for each dendritic location from all experiments were fitted with polynomial functions (5–7 order). The scale bars in *A* and *C* are 10 μm.

Comparison of $[Ca^{2+}]_i$ signals induced by the activation of α7 nAChRs and during depolarization

To estimate the relative efficiency of the α7 nAChRs to induce $[Ca^{2+}]_i$ changes in the dendrites of voltage-clamped neurons, we compared the $[Ca^{2+}]_i$ signals induced by the iontophoretic application of choline to those induced by depolarization to activate voltage-gated Ca^{2+} channels (VGCCs) (Fig. 4). When the membrane potential was depolarized from -70 mV to $+10$ mV for 100 ms, the increase in dendritic $[Ca^{2+}]_i$ level (93 ± 20 nM; 20 cells) was significantly larger ($P < 0.001$) than the $[Ca^{2+}]_i$ signals induced by the activation of α7-containing nAChRs in the dendrites (i.e. 34 nM; see above). Besides being significantly larger, the $[Ca^{2+}]_i$ signals induced by depolarization arose throughout the dendrite simultaneously, and were similar in amplitude along the dendrite (Fig. 4*A* and *B*). The kinetics of the depolarization-induced $[Ca^{2+}]_i$ signals were similar to the choline-induced $[Ca^{2+}]_i$ signals, with rise-time and half-time of decay values (for depolarization) of 0.26 ± 0.02 s and 2.1 ± 0.3 s, respectively.

$[Ca^{2+}]_i$ signals induced by α7 nAChR activation in dendrites are not due to Ca^{2+} intracellular store depletion, nor the activation of VGCCs

We tested whether the influx of Ca^{2+} directly through the α7 nAChRs is the major source of dendritic $[Ca^{2+}]_i$ signals, or whether other potential sources of Ca^{2+} might have been involved. Previously we found that the α7 nAChR-mediated $[Ca^{2+}]_i$ signals in the soma were not due to calcium-induced calcium release (CICR) from internal stores, nor the activation of VGCCs (Fayuk & Yakel, 2005). To test for the possible role of intracellular Ca^{2+} store depletion in generating the dendritic α7 nAChR-mediated $[Ca^{2+}]_i$ signals, slices were pretreated with ryanodine and cyclopiazonic acid (CPA). Ryanodine binds to ryanodine receptors, blocking the CICR from internal stores (McPherson *et al.* 1991). CPA, a selective blocker of sarcoplasmic–endoplasmic reticulum Ca^{2+}-ATPase (SERCA pumps; Seidler *et al.* 1989), was used to deplete the smooth endoplasmic reticulum-derived Ca^{2+} stores. After inducing an α7 nAChR-mediated response via the iontophoretic application of ACh to

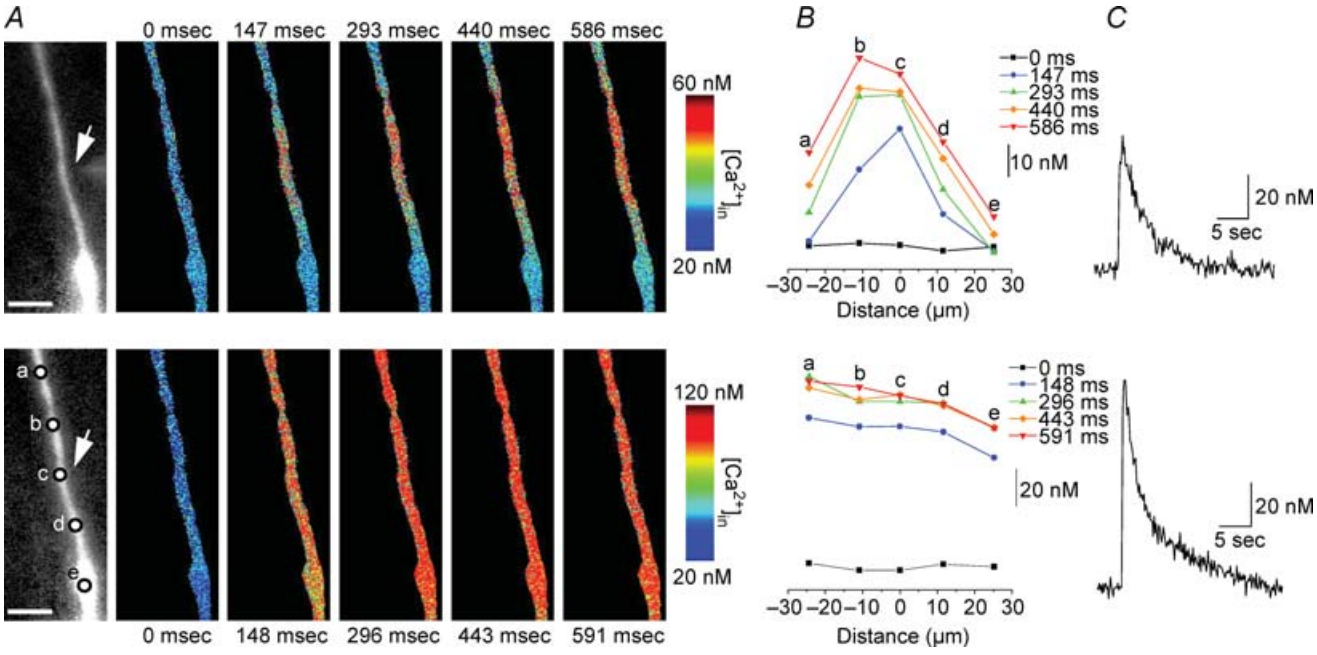

Figure 4. Comparison of dendritic $[Ca^{2+}]_i$ signals induced by α7 nAChR activation and during depolarization
A, series of pseudo-colour images of $[Ca^{2+}]_i$ signals in the same dendrite due to iontophoretic application of choline (top row), and due to depolarization (bottom row; from -70 mV to $+10$ mV for 100 ms). The arrow on the left fluorescence images depicts the location of the iontophoretic electrode; the scale bars are 10 μm. *B*, the time-dependent changes in $[Ca^{2+}]_i$ levels from five different locations for the dendrite in *A* (bottom left image). *C*, the $[Ca^{2+}]_i$ signals induced by choline (top) and depolarization (bottom) for the region nearest to the iontophoretic electrode (i.e. 'c').

dendrites, which resulted in $[Ca^{2+}]_i$ signals of 39 ± 20 nM (5 cells), ryanodine and CPA (both at 20 μM) were applied for 10 min; this treatment slowly increased $[Ca^{2+}]_i$ levels, which generally returned to baseline levels (data not shown). While in ryanodine and CPA, the amplitude of the α7 nAChR-mediated currents was significantly reduced (perhaps due to either rundown or partial block by ryanodine and CPA); however, neither the half-time of current decay nor the Ca^{2+} index value was significantly altered. In addition, the amplitude of the ACh-induced $[Ca^{2+}]_i$ signals was not significantly different (31 ± 9 nM in these same cells) after ryanodine and CPA treatment, which indicates that CICR does not significantly contribute to the peak amplitude of $[Ca^{2+}]_i$ signals observed in dendrites after activation of α7 nAChRs (Fig. 5). Interestingly, the half-time of decay of the $[Ca^{2+}]_i$ signals significantly increased after ryanodine and CPA treatment (from 2.5 ± 0.4 to 3.6 ± 0.3 s), suggesting that the recovery to resting $[Ca^{2+}]_i$ levels may have been affected by internal Ca^{2+} stores.

To test whether Ca^{2+} influx through VGCCs might have contributed to the α7 nAChR-mediated $[Ca^{2+}]_i$ signals, VGCCs were blocked with cadmium (Cd^{2+}; 200 μM). The application of Cd^{2+} before and during the activation of the α7 nAChRs did not significantly affect the dendritic ACh-induced $[Ca^{2+}]_i$ signals, which increased by 15 ± 3 nM before and 14 ± 2 nM during Cd^{2+} application in the same cells (5 cells). These data indicate that the activation of VGCCs does not significantly contribute to the $[Ca^{2+}]_i$ signals observed in dendrites after activation of α7 nAChRs under voltage-clamped conditions.

$[Ca^{2+}]_i$ signals in cultured hippocampal neurons due to the iontophoretic activation of α7 nAChRs

The major advantages of conducting imaging experiments in cultured neurons are that the soma and dendrites lie in the same focal plane, the distal dendrites can be more easily visualized, and the iontophoretic electrode can be quickly

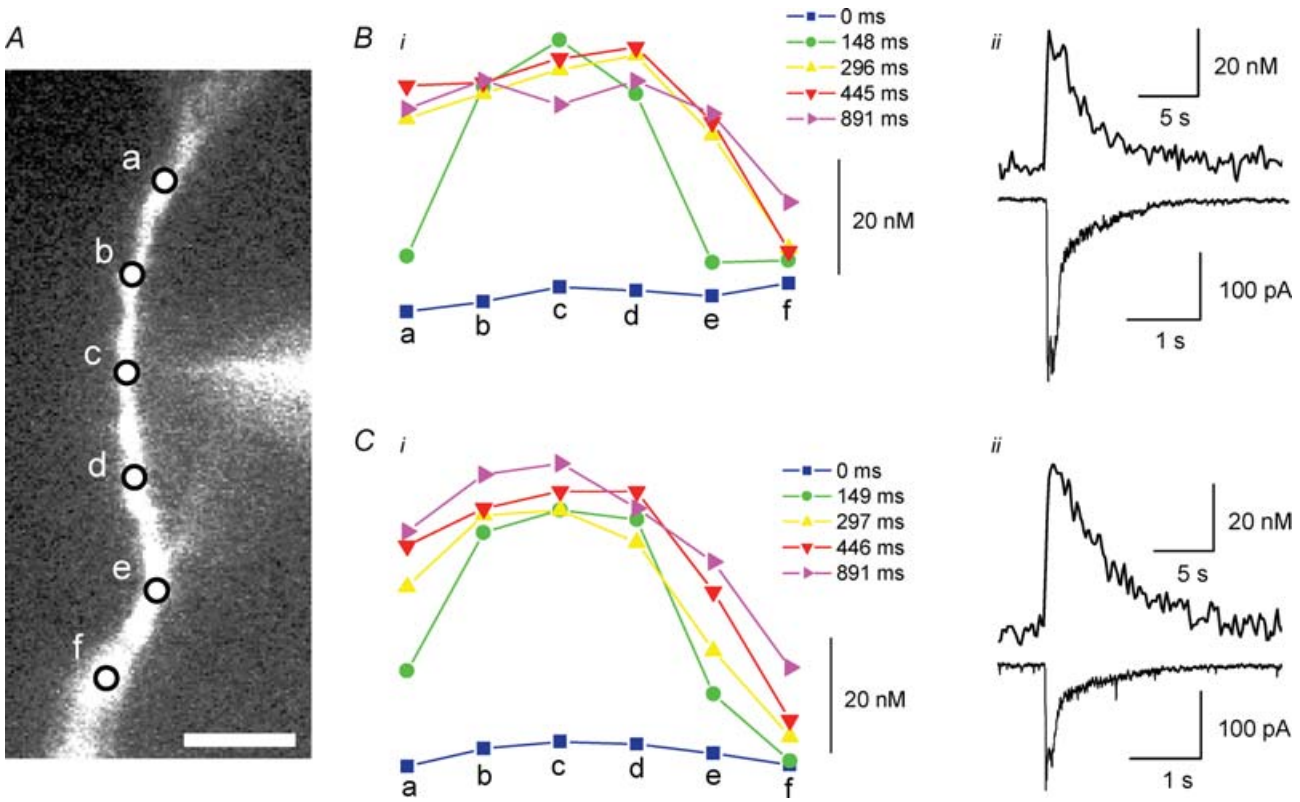

Figure 5. $[Ca^{2+}]_i$ signals induced by α7 nAChR activation in dendrites are not due to Ca^{2+} intracellular store depletion

A, fluorescence image with iontophoretic electrode in close proximity to the dendrite; the scale bar is 10 μm. *B*, the time-dependent changes in $[Ca^{2+}]_i$ levels due to α7 nAChR activation (under control conditions) from the six different locations denoted in *A*, with the $[Ca^{2+}]_i$ signal (*ii*, top) from the region nearest to the iontophoretic electrode (i.e. 'c' from the image in *A*) and current (*ii*, bottom). Note different time scale for top and bottom traces). *C*, time-dependent changes in $[Ca^{2+}]_i$ levels (same location as in *B*) after ryanodine and CPA (both at 20 μM, for 10 min) treatment (*i*), with the $[Ca^{2+}]_i$ signal (*ii*, top) and current (*ii*, bottom).

and easily located to any region of the cell. These factors allow for a broader study of the spatiotemporal dynamics of $[Ca^{2+}]_i$ signalling when compared to brain slices. Using brief iontophoretic application of choline (200 nA, 100 ms) to either the soma or dendrites of voltage-clamped cultured hippocampal neurons, we observed rapidly activating and decaying inward currents and $[Ca^{2+}]_i$ signals in 30% ($n = 56$ cells) of the cells tested that were similar to responses observed in slice recordings (Fig. 6). The average amplitude, rise-time and half-time of decay

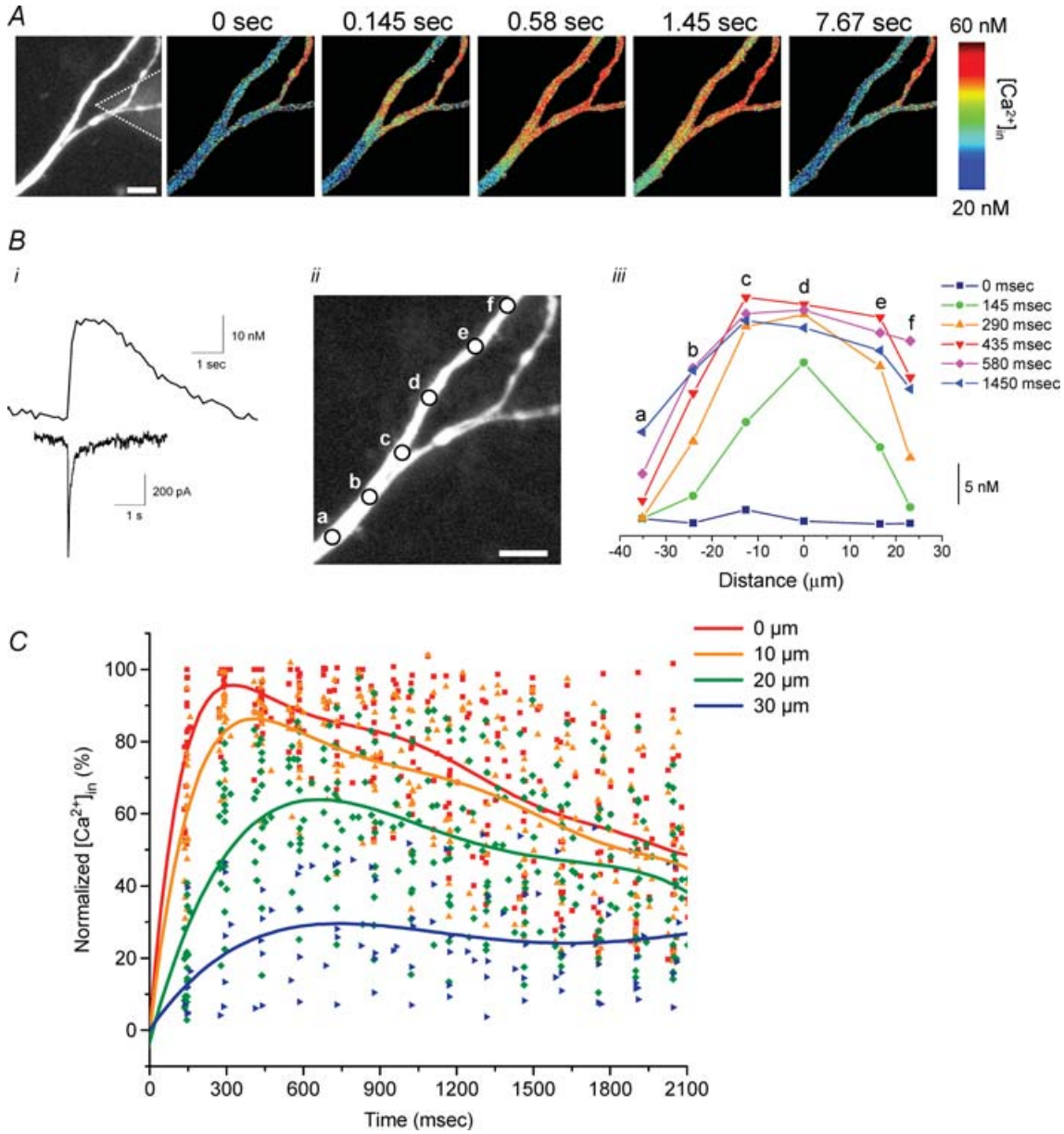

Figure 6. Iontophoretic activation of α7 nAChRs in cultured hippocampal neurons induces $[Ca^{2+}]_i$ signals similar to interneurons in slices

A, the iontophoretic application of choline to the dendrite of a cultured hippocampal neuron (fluorescence image on left shows the location of iontophoretic electrode by dotted lines; the scale bar is 10 μm) induced an increase in $[Ca^{2+}]_i$ levels as demonstrated by the pseudo-colour images. *B*, choline application induced a fast-activating and decaying inward current (bottom trace) and an increase in $[Ca^{2+}]_i$ levels (top trace; *i*); the $[Ca^{2+}]_i$ signal was from the region nearest to the iontophoretic electrode (i.e. 'd' from the image in *ii*). The time-dependent changes in $[Ca^{2+}]_i$ levels from six different locations for the dendrite (see *ii*) are shown in *iii*. *C*, summary of data obtained from similar experiments at 24 different locations in 5 cells. The changes in $[Ca^{2+}]_i$ levels for dendritic regions at variable distances (i.e. 0, 10, 20 and 30 μm) away from the tip of the iontophoretic electrode were plotted as a percentage of the maximal amplitude for the point nearest to the iontophoretic electrode (i.e. 0 μm) *versus* time after the iontophoretic application of choline. The data for each dendritic location from all experiments were fitted with polynomial functions (5–7 order). The scale bars in *A* and *Bii* are 10 μm.

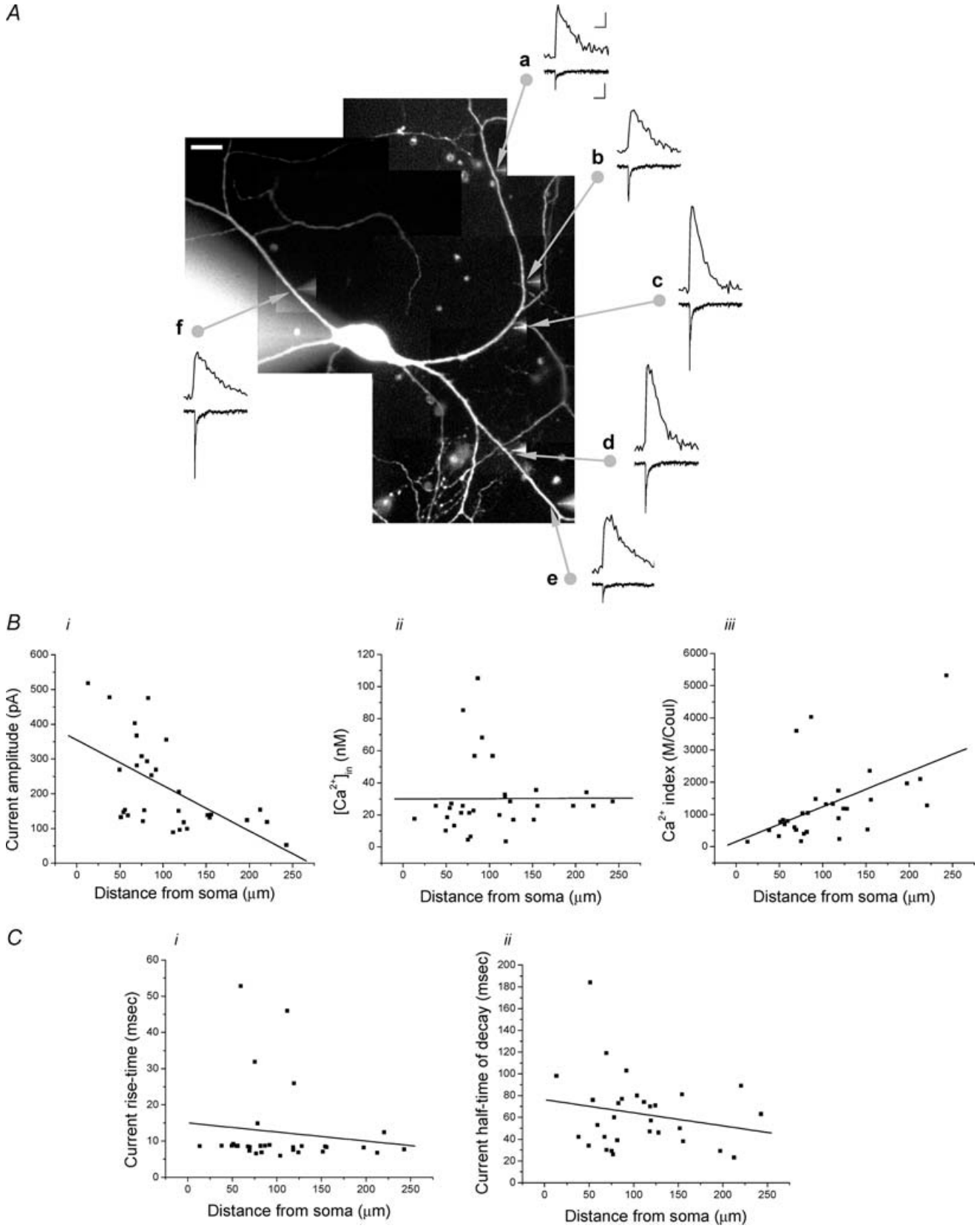

for currents in the soma were 516 ± 110 pA, 29 ± 7 ms and 179 ± 39 ms (5 cells), and for the dendrites these values were 218 ± 23 pA, 14 ± 2 ms and 71 ± 8 ms (17 cells; 41 different locations). The average amplitude, rise-time and half-time of decay for $[Ca^{2+}]_i$ signals in the soma were 5.3 ± 2 nM, 650 ± 100 ms and 5.0 ± 0.8 s (5 cells), and for the dendrites these values were 28 ± 3 nM, 310 ± 20 ms and 1.9 ± 0.2 s (17 cells; 41 different locations). As in slices, the α7 nAChR-induced currents were smaller and the decay kinetics faster in the dendrites of cultured hippocampal neurons, while the $[Ca^{2+}]_i$ signals were larger. The 'Ca^{2+} index' values for the soma and dendrites were 32 ± 5 M C^{-1} and 462 ± 140 M C^{-1}, respectively.

The temporal and spatial distribution of the dendritic α7 nAChR-mediated $[Ca^{2+}]_i$ signals in cultured neurons due to the iontophoretic application of choline was similar to what we observed in slices in that the $[Ca^{2+}]_i$ signals originated in the region nearest to the tip of the iontophoretic electrode and spread with decreasing amplitude along the dendrite in both directions away from the site of stimulation (Fig. 6). For the cell shown in Fig. 6, the $[Ca^{2+}]_i$ signals were measured at various points along the dendrite (Fig. 6*B*). A detectable $[Ca^{2+}]_i$ signal was already observed on the first image captured after choline application (i.e. 145 ms intervals; see Methods) for regions within ∼15 μm from the tip of the iontophoretic electrode (i.e. points 'c', 'd' and 'e'), with the largest signal for the region nearest the iontophoretic electrode (i.e. point 'd') that peaked by 290 ms (Fig. 6*B*). For locations further away, the peak of the $[Ca^{2+}]_i$ signal was delayed, and/or reached a lower peak level, consistent with the time and extent of diffusion of choline from the tip of the iontophoretic electrode.

We plotted the relative amplitude of the $[Ca^{2+}]_i$ signals (as a percentage of maximal response from the point nearest to the tip of the iontophoretic electrode) from 24 dendritic locations in five different cells *versus* time after the iontophoretic application of choline, for variable distances from the tip of the iontophoretic electrode (Fig. 6*C*). The $[Ca^{2+}]_i$ signals peaked in ∼300 ms for the region nearest the iontophoretic electrode, whereas at a distance of 10 μm, 20 μm and 30 μm, the $[Ca^{2+}]_i$ signals did not peak until ∼450 ms, 600 ms and 750 ms, respectively. The peak of the $[Ca^{2+}]_i$ signal also was decreased to ∼85%, 63% and 28%, respectively, at distances of 10 μm, 20 μm and 30 μm. These values were similar to those obtained in dendrites in slices.

In cultured hippocampal neurons, we also compared $[Ca^{2+}]_i$ signals induced by the iontophoretic application of choline to those induced by depolarization to activate VGCCs. Similar to slices, depolarization from −70 to +10 mV for 100 ms induced significantly larger $[Ca^{2+}]_i$ signals than choline application; the increase in $[Ca^{2+}]_i$ signals in the soma was 52 ± 6 nM (10 cells) and 66 ± 7 nM (14 cells) in the dendrites (these later two values were not significantly different). The rise-time and half-time of decay values for the depolarization-induced $[Ca^{2+}]_i$ signals in the soma were 0.46 ± 0.07 s and 6.1 ± 0.5 s (6 cells), and in the dendrites these values were 0.26 ± 0.04 s and 1.8 ± 0.2 s (7 cells); these kinetic values were not significantly different than for choline-induced $[Ca^{2+}]_i$ signals.

Functional mapping of α7 nAChR-mediated currents and $[Ca^{2+}]_i$ signals throughout the dendritic arbor of cultured hippocampal neurons

The distribution and function of the α7 nAChRs along the surface of the neurons is important to understand their physiological role in regulating neuronal excitability in the hippocampus. To address this issue, we studied inward currents and $[Ca^{2+}]_i$ signals induced by the iontophoretic application of choline at various places along the dendritic arbor of cultured hippocampal neurons (Fig. 7). We found that even though the amplitude of choline-induced currents decreased dramatically with distance away from the soma, the amplitude of the $[Ca^{2+}]_i$ signals did not appear to be dependent on distance from the soma (Fig. 7*A*). When we plotted the current amplitude *versus* distance from the soma (from ∼20 to 250 μm) from 31 dendritic locations in seven different cells, there was a clear negative correlation (Fig. 7*Bi*). This decrease in current amplitude is consistent with what was previously observed for the activation of α7 nAChRs by the local photolysis of caged carbachol in hippocampal slices (Khiroug *et al.* 2003). Despite this dramatic decrease in current amplitude

Figure 7. Distribution of functional α7 nAChR-mediated currents and $[Ca^{2+}]_i$ signals along the dendritic field in cultured hippocampal neurons

A, fluorescence image reconstruction of a cultured neuron with several dendrites; the scale bar is 10 μm. The iontophoretic application of choline to six different locations (arrows) throughout the dendritic field (points a–f) induced inward currents (scale bars are 100 pA and 1 s) and $[Ca^{2+}]_i$ signals (scale bars are 10 nM and 1 s) at each location. *B*, the amplitudes of inward current (*i*) and $[Ca^{2+}]_i$ signals (*ii*), and Ca^{2+} index values (*iii*) are plotted *versus* distance from the soma for 31 different dendritic locations in 7 different cells. The data were best approximated with linear regressions of the following parameters: for current amplitude, $r = -0.58$, $P < 0.001$; $[Ca^{2+}]_i$ signals, $r = 0.01$, $P > 0.95$; and Ca^{2+} index, $r = 0.52$, $P < 0.005$. *C*, the current rise-time (*i*) and half-time of decay values (*ii*) are plotted *versus* distance from the soma, with linear regressions of the following parameters: for rise-time, $r = -0.12$, $P > 0.50$; and for half-time of decay, $r = -0.20$, $P > 0.28$.

with distance, the amplitude of the $[Ca^{2+}]_i$ signals did not significantly change with distance from the soma (Fig. 7*Bii*). Therefore, the relative efficacy for the activation of α7 nAChRs to increase $[Ca^{2+}]_i$ levels (i.e. 'Ca^{2+} index' value) was several fold higher in the distal dendrites than proximal dendrites (Fig. 7*Biii*). There appeared to be no significant difference in the expression of functional α7 nAChRs between dendrites within the same cells.

We plotted the rise-time and half-time of decay values for currents *versus* distance from the soma to determine whether the decrease in current amplitude may have been attenuation due to filtering or space-clamp errors due to the cable properties of the dendrites (Fig. 7*C*). If this was occurring, there should have been significant decreases in the rise- and decay-time with increasing distance from the soma, as has been previously studied in dendritic recordings from hippocampal neurons (Spruston *et al.* 1993; Thurbon *et al.* 1994). However this was not the case since neither the rise-time (Fig. 7*Ci*) nor half-time of decay (Fig. 7*Cii*) values significantly changed with distance from the soma.

Discussion

Functional nAChRs in the hippocampus are known to be involved in cognition and working memory (Levin, 2002; Dani & Bertrand, 2007). A number of nAChR subtypes are permeable to Ca^{2+}, and therefore directly regulate $[Ca^{2+}]_i$ levels (Bertrand *et al.* 1993; Séguéla *et al.* 1993; Fucile, 2004), which in turn can regulate a variety of Ca^{2+}-dependent signal transduction cascades and synaptic plasticity (Berg & Conroy, 2002; Quick & Lester, 2002; Dajas-Bailador & Wonnacott, 2004; Fucile, 2004; Dani & Bertrand, 2007; Guo & Lester, 2007). The α7-containing receptors, the predominant nAChR subtype in hippocampal interneurons, are thought to be one of the most Ca^{2+} permeable (Jones *et al.* 1999; Fucile, 2004; Fayuk & Yakel, 2005). Previously we have shown that in the soma of rat hippocampal interneurons in slices, the activation of α7-containing nAChRs elicited significant but modest increases in $[Ca^{2+}]_i$ levels (Fayuk & Yakel, 2005). Here we have reported for the first time the spatiotemporal properties of the $[Ca^{2+}]_i$ signals and currents elicited by the rapid and local activation of α7-containing nAChRs in the dendrites of interneurons in hippocampal slices and cultured hippocampal neurons.

We have found that the amplitude of the $[Ca^{2+}]_i$ signals due to the iontophoretic application of choline was significantly larger in dendrites than in the soma in both slices and cultures, even though the amplitude of the inward currents was dramatically reduced in dendrites as compared to the soma. For the cultured hippocampal neurons, where the spatiotemporal dynamics of $[Ca^{2+}]_i$ signalling throughout the dendritic arbor could be more easily investigated, we showed that the relative efficacy for the α7 nAChR activation to increase $[Ca^{2+}]_i$ levels increased severalfold with distance away from the soma (from $\sim$20 to 250 μm).

We also demonstrated that the dendritic $[Ca^{2+}]_i$ signals induced by the iontophoretic application of choline, in either slices or cultures, were not due to Ca^{2+} intracellular store depletion (CICR), nor the activation of VGCCs, and therefore were probably due to the influx of Ca^{2+} directly through the α7 nAChRs. The relatively rapid rise-time and decay of currents and $[Ca^{2+}]_i$ signals is consistent with this notion. Similar to our studies, neither was found to participate in the nAChR-mediated current and $[Ca^{2+}]_i$ signals in rat medial habenula neurons (Guo & Lester, 2007). On the other hand, both CICR and the activation of VGCCs have previously been shown to participate in the nAChR-mediated increases in $[Ca^{2+}]_i$ levels in other native systems (Dajas-Bailador & Wonnacott, 2004).

Hippocampal interneurons can innervate and coordinate the activity of large numbers of principal neurons, and therefore have a powerful role in the regulation of hippocampal output via the organization of synchronous activity (Jones *et al.* 1999; Goldberg & Yuste, 2005). Although much knowledge has been acquired over the past decade relating to the dynamics of $[Ca^{2+}]_i$ signalling in the dendrites of pyramidal neurons in the hippocampus and neocortex, much less is known relating to $[Ca^{2+}]_i$ signals in interneurons. This is in part due to their highly heterogeneous nature and lack of easy classification, as well as to the technical difficulties associated with the smaller size of the dendrites (Goldberg & Yuste, 2005). Nevertheless, information regarding $[Ca^{2+}]_i$ signalling in dendrites is of great importance since dendrites serve a critical role in synapse integration. In addition, the electrical connectivity of interneurons indicates that the effects of synaptic integration can be significant over large areas (Goldberg & Yuste, 2005; Konur & Ghosh, 2005).

In rat hippocampal CA1 stratum radiatum interneurons, $[Ca^{2+}]_i$ signals induced by bAPs (back-propagating action potentials) or synaptic stimulation (both of which were due to the activation of VGCCs) increased in amplitude with distance from the soma, an effect that was not observed in pyramidal neurons (Rozsa *et al.* 2004). Furthermore, this gradient in $[Ca^{2+}]_i$ signals did not appear to be associated with significant changes in the Ca^{2+} buffering capacity along the dendrites, but appeared to be dependent on the dendritic geometry (i.e. diameter; Rozsa *et al.* 2004). The dramatic increase that we have observed in the relative efficacy of the α7 nAChR-mediated $[Ca^{2+}]_i$ signals with distance from the soma could also be a function of the dendritic geometry (e.g. due to the expected larger surface area-to-volume ratio of the distal dendrites) or differences in Ca^{2+} buffering capacity. However it is possible that other

mechanisms might be involved, including the differential distribution and/or regulation of various ion channels, pumps, or transporters. Lastly, the local environment around the mouth of the α7-containing nAChRs (e.g. the close association with elements that bind Ca^{2+}), as well as the regulation of the α7 nAChRs by Ca^{2+}-dependent processes, could alter $[Ca^{2+}]_i$ signals.

The decrease in amplitude of the α7 receptor-mediated currents, particularly in cultures where some currents were elicited more than 200 μm from the soma, may have been attenuated due to filtering or space-clamp errors due to the cable properties of the dendrites. The cable properties of hippocampal neurons, particular in slices, have been well-studied both in pyramidal neurons and in interneurons. Spruston *et al.* (1993) studied voltage- and space-clamp errors in CA3 pyramidal neurons in slices. They estimated (under similar conditions to those utilized here) that the voltage attenuation in dendrites at a distance of 250 μm from the soma would have resulted in errors of less than 5 mV. This small voltage error is much too small to explain the severalfold decrease in current amplitude that we have observed here. However, there still could be significant attenuation of the current signals due to membrane capacitance and internal resistance; any attenuation would be accompanied by significant decreases in both the rise- and decay-time of responses with increasing distance from the soma (Spruston *et al.* 1993). In slices from the hippocampal CA1 region, interneurons were shown to have similar electrotonic profiles to pyramidal neurons (Thurbon *et al.* 1994). In addition, the much faster AMPA receptor-mediated synaptic currents were attenuated and slowed down much more (as expected) than the slower NMDA receptor-mediated synaptic currents in interneurons. The fact that we observed that neither the rise-time nor the half-time of decay values significantly changed with distance from the soma in cultured neurons suggests that for the α7 nAChR-mediated responses studied here, there was little to no significant attenuation of current amplitudes. Lastly as we previously reported (Khiroug *et al.* 2003), the decrease in amplitude of the α7 receptor-mediated responses with distance from the soma was much greater than for glutamate receptor-mediated responses, suggesting further that the decrease is unlikely to be due to dendritic filtering, but rather to be due to actual differences in relative expression of receptors between the soma and dendrites.

The increases in $[Ca^{2+}]_i$ levels due to the influx of Ca^{2+} through the α7 nAChRs that we have observed in both dendrites and soma might be sufficient to regulate these channels either directly, or through Ca^{2+}-dependent signal transduction cascades. We previously have shown that the rate of recovery from desensitization of these α7 receptors is regulated by $[Ca^{2+}]_i$ (Khiroug *et al.* 2003), and we recently described a novel form of potentiation of these α7-containing nAChRs that was regulated by Ca^{2+}, and Ca^{2+}-dependent cascades involving calcineurin, PKC, and/or CaMKII (Klein & Yakel, 2005). Besides regulating ion channel function and neuronal excitability, the influx of Ca^{2+} through the α7 receptors might also regulate other processes such as neurotransmitter release, gene expression, cell proliferation, survival and death, and development (Role & Berg, 1996; Dajas-Bailador & Wonnacott, 2004). For example in chick ciliary ganglion (CG) neurons, the activation of α7-containing nAChRs induces Ca^{2+} influx, which activates the CaMK and MAPK pathways, leading to activation of the transcription factor CREB and gene expression; however, this happens only if the VGCCs fail to open (Chang & Berg, 2001). In addition it was also recently shown in chick CG neurons that the transition from GABA-induced excitation to inhibition during development is in part due to the activation of the α7-containing nAChRs, demonstrating that nAChR activation is important for development (Liu *et al.* 2006). Finally in both rodent hippocampal interneurons and chick CG neurons, Ca^{2+} influx through the α7-containing nAChRs down-regulates $GABA_A$ receptor-induced currents via a CaMK- and MAPK-dependent pathway (Zhang & Berg, 2007). Therefore Ca^{2+}, and in particular Ca^{2+} influx through α7 nAChRs, can regulate a variety of signal transduction cascades. However, the precise spatiotemporal dynamics of the $[Ca^{2+}]_i$ signals are critical in determining what affect this will have on ion channel regulation, various forms of synaptic plasticity, gene expression, as well as excitability. For example in rat hippocampal CA1 stratum oriens/alveus interneurons, the activation of both ionotropic and metabotropic glutamate receptors produces different $[Ca^{2+}]_i$ signals at different dendritic sites, which can serve distinct signalling functions and therefore allow for multiple forms of synaptic plasticity (Topolnik *et al.* 2005). In addition, local $[Ca^{2+}]_i$ signals can affect neuronal morphology by regulating the growth and branching of dendrites, perhaps through modulation of the cytoskeleton near the point of Ca^{2+} entry (Konur & Ghosh, 2005).

In conclusion, we have shown that for both rat hippocampal interneurons in slices and cultured rat hippocampal neurons, the local activation of the α7-containing nAChRs induces $[Ca^{2+}]_i$ signals significantly larger in dendrites than the soma, even though the amplitude of the currents was significantly smaller. In addition in cultured neurons, even though the amplitude of the α7 nAChR-mediated currents dramatically decreased with distance from the soma, surprisingly the amplitude of the $[Ca^{2+}]_i$ signals was unchanged. These results may have implications for the heterogeneous functional roles that α7 nAChRs may play in the soma or dendrites via changes in $[Ca^{2+}]_i$ levels, and in regulating a variety of signal transduction cascades, synaptic plasticity, and memory processes.

References

Berg DK & Conroy WG (2002). Nicotinic $\alpha 7$ receptors: synaptic options and downstream signaling in neurons. *J Neurobiol* **53**, 512–523.

Bertrand D, Galzi JL, Devillers-Thiéry A, Bertrand S & Changeux J-P (1993). Mutations at two distinct sites within the channel domain M2 alter calcium permeability of neuronal $\alpha 7$ nicotinic receptor. *Proc Natl Acad Sci U S A* **90**, 6971–6975.

Castro NG & Albuquerque EX (1995). α-Bungarotoxin-sensitive hippocampal nicotinic receptor channel has a high calcium permeability. *Biophys J* **68**, 516–524.

Chang KT & Berg DK (2001). Voltage-gated channels block nicotinic regulation of CREB phosphorylation and gene expression in neurons. *Neuron* **32**, 855–865.

Dajas-Bailador F & Wonnacott S (2004). Nicotinic acetylcholine receptors and the regulation of neuronal signaling. *Trends Pharmacol Sci* **25**, 317–324.

Dani JA & Bertrand D (2007). Nicotinic acetylcholine receptors and nicotinic cholinergic mechanisms of the central nervous system. *Annu Rev Pharmacol Toxicol* **47**, 699–729.

Engel AG & Sine SM (2005). Current understanding of congenital myasthenic syndromes. *Current Opin Pharmacol* **5**, 308–321.

Fayuk D & Yakel JL (2004). Regulation of nicotinic acetylcholine receptor channel function by acetylcholinesterase inhibitors in rat hippocampal CA1 interneurons. *Mol Pharmacol* **66**, 658–666.

Fayuk D & Yakel JL (2005). Ca^{2+} permeability of nicotinic acetylcholine receptors in rat hippocampal CA1 interneurons. *J Physiol* **566**, 759–768.

Frotscher M & Léránth C (1985). Cholinergic innervation of the rat hippocampus as revealed by choline acetyltransferase immunocytochemistry: a combined light and electron microscopic study. *J Comp Neurol* **239**, 237–246.

Fucile S (2004). Ca^{2+} permeability of nicotinic acetylcholine receptors. *Cell Calcium* **35**, 1–8.

Fucile S, Sucapane A, Grassi F, Eusebi F & Engel AG (2006). The human adult subtype ACh receptor channel has high Ca^{2+} permeability and predisposes to endplate Ca^{2+} overloading. *J Physiol* **573**, 35–43.

Fujii S & Sumikawa K (2001). Nicotine accelerates reversal of long-term potentiation and enhances long-term depression in the rat hippocampal CA1 region. *Brain Res* **894**, 340–346.

Goldberg JH & Yuste R (2005). Space matters: local and global dendritic Ca^{2+} compartmentalization in cortical interneurons. *Trends Neurosci* **28**, 158–167.

Guo X & Lester RA (2007). Ca^{2+} flux and signaling implications by nicotinic acetylcholine receptors in rat medial habenula. *J Neurophysiol* **97**, 83–92.

Hu M, Liu QS, Chang KT & Berg DK (2002). Nicotinic regulation of CREB activation in hippocampal neurons by glutamatergic and nonglutamatergic pathways. *Mol Cell Neurosci* **21**, 616–625.

Hunter BE, de Fiebre CM, Papke RL, Kem WR & Meyer EM (1994). A novel nicotinic agonist facilitates induction of long-term potentiation in the rat hippocampus. *Neurosci Lett* **168**, 130–134.

Ji D, Lape R & Dani JA (2001). Timing and location of nicotinic activity enhances or depresses hippocampal synaptic plasticity. *Neuron* **31**, 131–141.

Jones S, Sudweeks S & Yakel JL (1999). Nicotinic receptors in the brain: correlating physiology with function. *Trends Neurosci* **22**, 555–561.

Khiroug L, Giniatullin R, Klein RC, Fayuk D & Yakel JL (2003). Functional mapping and Ca^{2+} regulation of nicotinic acetylcholine receptor channels in rat hippocampal CA1 neurons. *J Neurosci* **23**, 9024–9031.

Klein RC & Yakel JL (2005). Paired-pulse potentiation of $\alpha 7$-containing nAChRs in rat hippocampal CA1 stratum radiatum interneurones. *J Physiol* **568**, 881–889.

Konur S & Ghosh A (2005). Calcium signaling and the control of dendritic development. *Neuron* **46**, 401–405.

Levin ED (2002). Nicotinic receptor subtypes and cognitive function. *J Neurobiol* **53**, 633–640.

Liu Q & Berg DK (1999). Actin filaments and the opposing actions of CaM kinase II and calcineurin in regulating $\alpha 7$-containing nicotinic receptors on chick ciliary ganglion neurons. *J Neurosci* **19**, 10280–10288.

Liu Z, Neff RA & Berg DK (2006). Sequential interplay of nicotinic and GABAergic signaling guides neuronal development. *Science* **314**, 1610–1613.

Liu Z, Tearle AW, Nai Q & Berg DK (2005). Rapid activity-driven SNARE-dependent trafficking of nicotinic receptors on somatic spines. *J Neurosci* **25**, 1159–1168.

Lukas RJ, Lucero L, Buisson B, Galzi JL, Puchacz E, Fryer JD, Changeux JP & Bertrand D (2001). Neurotoxicity of channel mutations in heterologously expressed $\alpha 7$-nicotinic acetylcholine receptors. *Eur J Neurosci* **13**, 1849–1860.

McGehee DS (2002). Nicotinic receptors and hippocampal synaptic plasticity . . . it's all in the timing. *Trends Neurosci* **25**, 171–172.

McPherson PS, Kim YK, Valdivia H, Knudson CM, Takekura H, Franzini-Armstrong C, Coronado R & Campbell KP (1991). The brain ryanodine receptor: a caffeine-sensitive calcium release channel. *Neuron* **7**, 17–25.

Papke RL, Bencherif M & Lippiello P (1996). An evaluation of neuronal nicotinic acetylcholine receptor activation by quaternary nitrogen compounds indicates that choline is selective for the $\alpha 7$ subtype. *Neurosci Lett* **213**, 201–204.

Quick MW & Lester RA (2002). Desensitization of neuronal nicotinic receptors. *J Neurobiol* **53**, 457–478.

Role LW & Berg DK (1996). Nicotinic receptors in the development and modulation of CNS synapses. *Neuron* **16**, 1077–1085.

Rozsa B, Zelles T, Vizi ES & Lendvai B (2004). Distance-dependent scaling of calcium transients evoked by backpropagating spikes and synaptic activity in dendrites of hippocampal interneurons. *J Neurosci* **24**, 661–670.

Séguéla P, Wadiche J, Dineley-Miller K, Dani JA & Patrick JW (1993). Molecular cloning, functional properties, and distribution of rat brain $\alpha 7$: a nicotinic cation channel highly permeable to calcium. *J Neurosci* **13**, 596–604.

Seidler NW, Jona I, Vegh M & Martonosi A (1989). Cyclopiazonic acid is a specific inhibitor of the Ca^{2+}-ATPase of sarcoplasmic reticulum. *J Biol Chem* **264**, 17816–17823.

Spruston N, Jaffe DB, Williams SH & Johnston D (1993). Voltage- and space-clamp errors associated with the measurement of electrotonically remote synaptic events. *J Neurophysiol* **70**, 781–802.

Thurbon D, Field A & Redman S (1994). Electrotonic profiles of interneurons in stratum pyramidale of the CA1 region of rat hippocampus. *J Neurophysiol* **71**, 1948–1958.

Topolnik L, Congar P & Lacaille JC (2005). Differential regulation of metabotropic glutamate receptor- and AMPA receptor-mediated dendritic Ca^{2+} signals by presynaptic and postsynaptic activity in hippocampal interneurons. *J Neurosci* **25**, 990–1001.

Woolf NJ (1991). Cholinergic systems in mammalian brain and spinal cord. *Prog Neurobiol* **37**, 474–524.

Zhang J & Berg DK (2007). Reversible inhibition of $GABA_A$ receptors by α7-containing nicotinic receptors on the postsynaptic neuron. *J Physiol* **579**, 753–763.

Acknowledgements

We would like to thank C. Erxleben and S. Gentile for advice in preparing the manuscript, and Rachel Robinson for preparing cell cultures. The research was supported by the Intramural Research Program of the NIH, National Institute of Environmental Health Sciences.